



1 **Identification of hydrological model parameters variation using**
2 **ensemble Kalman filter**

3

4 Chao Deng^{1,2}, Pan Liu^{1,2,*}, Shenglian Guo^{1,2}, Zejun Li^{1,2}, Dingbao Wang³

5

6 ¹State Key Laboratory of Water Resources and Hydropower Engineering Science, Wuhan University,
7 Wuhan, China

8 ²Hubei Provincial Collaborative Innovation Center for Water Resources Security, Wuhan, China

9 ³Department of Civil, Environmental & Construction Engineering, University of Central Florida,
10 Orlando, USA

11

12 *Corresponding author: P. Liu, State Key Laboratory of Water Resources and Hydropower

13 Engineering Science, Wuhan University, Wuhan 430072, China

14 Email: liupan@whu.edu.cn

15 Tel: +86-27-68775788; Fax: +86-27-68773568



16 **Abstract:** Hydrological model parameters play an important role in the ability of model prediction. In
17 a stationary content, parameters of hydrological models are treated as constants. However, model
18 parameters may vary dynamically with time under climate change and human activities. The technique
19 of ensemble Kalman filter (EnKF) is proposed to identify the temporal variation of parameters for a
20 two-parameter monthly water balance model by assimilating the runoff observations, where one of state
21 equations is that the model parameters should not change much within a short time period. Through a
22 synthetic experiment, the proposed method is evaluated with various types of parameter variations
23 including trend, abrupt change, and periodicity. The application of the method to the Wudinghe basin
24 shows that the water storage capacity, a parameter in the model, has an apparent increasing trend during
25 the period from 1958 to 2000. The identified temporal variation of water storage capacity is explained
26 by land use and land cover changes due to soil and water conservation measurements. Whereas, the
27 application to the Tongtianhe basin demonstrates that the parameter of water storage capacity has no
28 significant variation during the simulation of 1982-2013, corresponding to the relatively stationary
29 catchment characteristics. Additionally, the proposed method improves the performance of hydrological
30 modeling, and provides an effective tool for quantifying temporal variation of model parameters.

31

32 **Keywords:** model parameter identification, temporal variation of parameter, catchment characteristics,
33 ensemble Kalman filter



34 **1 Introduction**

35 Hydrological model parameters are critically important for accurate simulation of streamflow. In
36 hydrological modeling, parameters are usually assumed to be stationary, i.e., the calibrated parameters
37 are a set of constants during the calibration period, and have extrapolative ability outside the range of
38 the observations used for parameter estimation (Merz et al., 2011). However, the calibration period may
39 contain different climactic condition and hydrological regime, and has a significant impact on the model
40 parameter estimation (Merz et al., 2011; Zhang et al., 2011; Westra et al., 2014; Patil and Stieglitz,
41 2015). The model parameters may potentially change responding to time-variable precipitation and
42 other inputs. For example, land use and land cover changes contribute to temporal change of model
43 parameters (Andréassian et al., 2003; Brown et al., 2005; Merz et al., 2011). Consequently, assuming
44 time invariant model parameters may be unrealistic, especially for catchments with time-varying
45 climate conditions and/or catchment properties.

46

47 The situation of time-variant hydrological model parameters has been reported in a few publications
48 (Merz et al., 2011; Brigode et al., 2013; Westra et al., 2014; Patil and Stieglitz, 2015). For example, Ye
49 et al. (1997) and Paik et al. (2005) mentioned the seasonal variations of hydrological model parameters.
50 Merz et al. (2011) analyzed the temporal changes of model parameters which were calibrated
51 respectively by using six consecutive 5 year periods between 1976 and 2006 for 273 catchments in



52 Austria. Recently, Westra et al. (2014) proposed a strategy to cope with nonstationary of hydrological
53 model parameters, which were represented as a function of a set of time-varying covariates before using
54 an optimization algorithm for calibration. Previous studies provided two main methods to identify the
55 time-variant model parameters: (1) Divide the historical record into consecutive subsets, and then
56 calibrate the model parameters using an optimization algorithm (e.g., Merz et al. (2011)). The model
57 parameters are fixed values in each subset. (2) Build the functional form of the selected time-variant
58 model parameters, and calibrate the model parameters using an optimization algorithm based on the
59 entire historical record (e.g., Westra et al. (2014)).

60

61 The data assimilation (DA) method has been used to estimate both model parameters and state variables.
62 For example, Vrugt et al. (2013) proposed two types of Particle-DREAM method to track the evolving
63 target distribution of model parameters. Although the DA method has been used to estimate model
64 parameters, the objective is to identify the fixed values of parameters. Additionally, little attention has
65 been paid to the identification of time-variant model parameters and the interpretation of their temporal
66 variations based on the climate conditions and/or catchment characteristics.

67

68 The aim of this study is to assess the capability of the DA method (i.e., the EnKF) to identify the
69 temporal variation of parameters for a monthly water balance model, and to link the parameter



70 variations to changes in physical properties.

71

72 The remainder of this paper is organized as follows. Section 2 presents a brief review of the
73 two-parameter monthly water balance model and the EnKF method. Following the methodology,
74 Section 3 describes the synthetic experiment and the application to two case studies. Results and
75 discussion are presented in Section 4, followed by conclusions in Section 5.

76

77 **2 Methodology**

78 **2.1 Monthly water balance model**

79 The two-parameter monthly water balance model, developed by Xiong and Guo (1999), has been
80 widely applied for monthly runoff simulation and forecast (Guo et al., 2002; Guo et al., 2005; Xiong
81 and Guo, 2012; Li et al., 2013; Zhang et al., 2013; Xiong et al., 2014). The inputs of the model include
82 monthly areal precipitation and potential evapotranspiration. The actual monthly evapotranspiration is
83 calculated as follows:

$$84 \quad E_i = C \times EP_i \times \tanh(P_i / EP_i) \quad (1)$$

85 where E_i represents the actual monthly evapotranspiration; EP_i and P_i are the monthly potential
86 evapotranspiration and precipitation, respectively; C is the first model parameter; and i is the time
87 step.



88

89 The monthly runoff is dependent on the soil water content and is calculated by the following formula:

$$90 \quad Q_i = S_i \times \tanh(S_i / SC) \quad (2)$$

91 where Q_i is the monthly runoff; and S_i is the soil water content. As the second model parameter,

92 SC represents the water storage capacity of the catchment with the unit of millimeter. The available

93 water for runoff at the i th month is computed by $S_{i-1} + P_i - E_i$. Then, the monthly runoff is calculated

94 by:

$$95 \quad Q_i = (S_{i-1} + P_i - E_i) \times \tanh[(S_{i-1} + P_i - E_i) / SC] \quad (3)$$

96

97 Finally, the soil water content at the end of each time step is updated based on the water conservation

98 law:

$$99 \quad S_i = S_{i-1} + P_i - E_i - Q_i \quad (4)$$

100

101 **2.2 Ensemble Kalman filter**

102 EnKF is a sequential data assimilation technique based on the Monte Carlo method and produces an

103 ensemble of state simulations to update the state variables and model parameters, conditioned on a

104 series of model observations (Moradkhani et al., 2005; Shi et al., 2014). It has been successfully

105 applied into dozens of hydrological applications (Abaza et al., 2014; DeChant and Moradkhani, 2014;



106 Delijani et al., 2014; Samuel et al., 2014; Tamura et al., 2014; Xue and Zhang, 2014; Deng et al.,
107 2015). In EnKF, the state equation is as follows:

$$108 \quad \theta_{i+1} = \theta_i + \delta_i, \delta_i \sim N(0, R_i) \quad (5)$$

$$109 \quad x_{i+1} = f(x_i, \theta_{i+1}) + \varepsilon_i, \varepsilon_i \sim N(0, G_i) \quad (6)$$

110 where x_i is the state vector with a dimension of $n \times 1$ at time i ; θ_{i+1} is the parameter vector with a
111 dimension of $l \times 1$ at time $i+1$; f is the forward operator; ε_i and δ_i are the independent white
112 noise for the forecast model with a dimension of $n \times 1$, followed a Gaussian distribution with zero
113 mean and covariance matrix G_i and R_i with a dimension of $n \times n$, respectively. Equation (5)
114 indicates that hydrological parameters should not change much within a short time period.

115

116 The observation equation is as follows:

$$117 \quad y_{i+1} = h(x_{i+1}, \theta_{i+1}) + \xi_{i+1}, \xi_{i+1} \sim N(0, S_{i+1}) \quad (7)$$

118 where y_{i+1} is the observation vector with a dimension of $m \times 1$ at time $i+1$; h is the
119 observational operator which represents the relationship between the observations and states; ξ_{i+1} is
120 the noise term with a dimension of $m \times 1$ which follows a Gaussian distribution with zero mean and
121 covariance matrix S_{i+1} with a dimension of $m \times m$.

122

123 Based on the available state and observation equations, the EnKF assimilation process can be



124 expressed as follows:

125 (1) Set the ensemble size N and the total length of the historical record n .

126 (2) Generate the ensemble of model parameters and state variables by perturbing the updated values
 127 from the previous time step.

$$128 \quad \theta_{i+1|i}^k = \theta_{i|i}^k + \delta_i^k \quad (8)$$

$$129 \quad x_{i+1|i}^k = f\left(x_{i|i}^k, \theta_{i+1|i}^k\right) + \varepsilon_i^k \quad (9)$$

130 where $\theta_{i+1|i}^k$ is the k th ensemble member forecast at time $i+1$; $\theta_{i|i}^k$ is the k th updated ensemble
 131 member at time i ; δ_i is the white noise for the k th ensemble member; $x_{i+1|i}^k$ is the k th ensemble
 132 member forecast at time $i+1$; $x_{i|i}^k$ is the k th updated ensemble member at time i ; and ε_i^k is the
 133 white noise for the k th ensemble member.

134 (3) Generate the ensemble of runoff observations by adding a perturbation:

$$135 \quad y_{i+1}^k = y_{i+1} + \xi_{i+1}^k \quad (10)$$

136 where y_{i+1}^k is the k th observation ensemble member at time $i+1$; and ξ_{i+1}^k is the observation error
 137 for the k th ensemble member.

138

139 The model parameters and state variables are updated according to the following equations:

$$140 \quad x_{i+1|i+1}^k = x_{i+1|i}^k + K_{i+1}^x \left(y_{i+1}^k - h\left(x_{i+1|i}^k, \theta_{i+1|i}^k\right) \right) \quad (11)$$

$$141 \quad \theta_{i+1|i+1}^k = \theta_{i+1|i}^k + K_{i+1}^\theta \left(y_{i+1}^k - h\left(x_{i+1|i}^k, \theta_{i+1|i}^k\right) \right) \quad (12)$$



142

143 Note that the parameter and state vectors are updated following the approach in the previous studies
 144 (Wang et al., 2009; Nie et al., 2011; DeChant and Moradkhani, 2012; Lü et al., 2013). K_{i+1} is the
 145 Kalman gain matrix that represents the weight between the forecasts and observations. It can be
 146 calculated by (Moradkhani et al., 2005):

$$147 \quad K_{i+1}^x = \sum_{i+1|i}^{xy} \left(\sum_{i+1|i}^{yy} + S_{i+1} \right)^{-1} \quad (13)$$

$$148 \quad K_{i+1}^\theta = \sum_{i+1|i}^{\theta y} \left(\sum_{i+1|i}^{yy} + S_{i+1} \right)^{-1} \quad (14)$$

$$149 \quad \sum_{i+1|i}^{xy} = \frac{1}{N-1} X_{i+1|i} Y_{i+1|i}^T \quad (15)$$

$$150 \quad \sum_{i+1|i}^{\theta y} = \frac{1}{N-1} \Theta_{i+1|i} Y_{i+1|i}^T \quad (16)$$

$$151 \quad \sum_{i+1|i}^{yy} = \frac{1}{N-1} Y_{i+1|i} Y_{i+1|i}^T \quad (17)$$

152 where $\sum_{i+1|i}^{xy}$ is the cross covariance of the forecasted states; $\sum_{i+1|i}^{\theta y}$ is the cross covariance of the forecasted
 153 parameters; $\sum_{i+1|i}^{yy}$ is the error covariance of the forecasted output; $X_{i+1|i} = \left(x_{i+1|i}^1 - x_{i+1|i}^m, \dots, x_{i+1|i}^N - x_{i+1|i}^m \right)$ and $x_{i+1|i}^m$
 154 is the ensemble mean of the forecasted states; $\Theta_{i+1|i} = \left(\theta_{i+1|i}^1 - \theta_{i+1|i}^m, \dots, \theta_{i+1|i}^N - \theta_{i+1|i}^m \right)$ and $\theta_{i+1|i}^m$ is the ensemble mean
 155 of the forecasted parameters; $Y_{i+1|i} = \left(y_{i+1|i}^1 - y_{i+1|i}^m, \dots, y_{i+1|i}^N - y_{i+1|i}^m \right)$ and $y_{i+1|i}^m$ is the ensemble mean of the
 156 forecasted output; N is the number of ensemble members; and the superscript T represents the matrix transpose.
 157 Since the parameters are limited within an interval, the constrained EnKF is used (Wang et al., 2009) in this study.

158

159 The ensemble size, uncertainties in input and output have significant impacts on the assimilation



160 performance of the EnKF, and they are determined based on previous studies (Wang et al., 2009; Xie
161 and Zhang, 2010; Lü et al., 2013; Samuel et al., 2014). The ensemble size is set to 1000 for all cases.
162 In the present study, the uncertainties including parameter errors (ε , Eq. (8)), state variable error (δ ,
163 Eq. (9)) and streamflow observation error (ξ , Eq. (10)), are assumed to follow a Gaussian distribution.
164 In terms of the parameter errors, the standard deviation for C is set to 0.01 for all the cases, while
165 that of SC are set from 0.5 to 5 to account for its uncertainties. The standard deviation of both model
166 state and observation errors are assumed to be proportional to the magnitude of true values, and the
167 scale factors are set to be 5% and 10% respectively for all cases (Wang et al., 2009; Lü et al., 2013). It
168 should be noted that the variable variance multiplier can be used to perturb the observations
169 (Leisenring and Moradkhani, 2012; Yan et al., 2015).

170

171 **2.3 Evaluation index**

172 Two evaluation criteria, including the Nash-Sutcliffe efficiency (NSE) (Nash and Sutcliffe, 1970) and
173 the volume error (VE) are used to evaluate the runoff assimilation results for the synthetic experiment
174 and application to catchments (Deng et al., 2015; Li et al., 2015).

$$175 \quad NSE = 1 - \frac{\sum_{i=1}^n (Q_{sim,i} - Q_{obs,i})^2}{\sum_{i=1}^n (Q_{obs,i} - \bar{Q}_{obs})^2} \quad (18)$$



176
$$VE = \frac{\sum_{i=1}^n Q_{sim,i} - \sum_{i=1}^n Q_{obs,i}}{\sum_{i=1}^n Q_{obs,i}} \quad (19)$$

177 where $Q_{sim,i}$ and $Q_{obs,i}$ are the simulated and observed runoff for the i th month; \bar{Q}_{sim} and \bar{Q}_{obs}
178 are the mean of the simulated and observed runoff, respectively for the i th month; and n is the total
179 number of data points. The NSE has been widely used to assess the goodness-of-fit for hydrological
180 modeling. A NSE value of 1 means a perfect match of simulated runoff to the observations. The VE is
181 a measure of bias between the simulated and observed runoff. For example, VE with the value of 0
182 denotes no bias, and a negative value means an underestimation of the total runoff volume.

183

184 **3 Data and study area**

185 **3.1 Synthetic experiment**

186 A synthetic experiment is designed to evaluate the capability of the assimilation procedure to identify
187 the temporal variation of model parameters. The model parameters are given with specific variation
188 including trend, abrupt change and periodicity. Observations for precipitation and potential
189 evapotranspiration are generated via a stochastic simulation, and runoff is then produced by using the
190 monthly water balance model. The steps toward identifying temporal variation of model parameters are
191 as follows:

192 (1) Scenarios set: Generate the time-variant parameters with different trend variations, potential
193 evapotranspiration and precipitation on a monthly time scale, then compute the runoff observations



194 using the two-parameter monthly water balance model.

195 (2) Initialization: Specify the ensemble size and the total number of assimilation time steps. At the first
196 time step, the model parameter and state variable ensembles are generated using a predefined Gaussian
197 distribution based on the prior intervals in **Table 1**.

198 (3) Data assimilation: After the initialization of parameters and state variables, the hydrologic model
199 parameters and state are updated by assimilating the runoff observations obtained in Step (1). Note that
200 the model parameters and state, as well as the runoff observations, are perturbed with an error item
201 which is assumed a Gaussian distribution with zero mean and specified variance.

202

203 The data set used in this experiment has a total length of 672 months. The first 24 months is set as
204 model warm-up period to reduce the impact of the initial hydrological conditions. The experiment is
205 implemented to identify the variation of model parameters from the scenarios in **Table 2**, respectively.

206

207 The assimilated parameter results are evaluated using the following criteria, including the Pearson
208 correlation coefficient (R), the root mean square error (RMSE) and mean absolute relative error
209 (MARE):

210

$$R = \frac{\sum_{i=1}^n (x_{sim,i} - \bar{x}_{sim})(x_{obs,i} - \bar{x}_{obs})}{\sqrt{\sum_{i=1}^n (x_{sim,i} - \bar{x}_{sim})^2 (x_{obs,i} - \bar{x}_{obs})^2}} \quad (20)$$



211
$$RMSE = \sqrt{\frac{1}{n} \sum_{i=1}^n (x_{sim,i} - x_{obs,i})^2}$$
 (21)

212
$$MARE = \frac{1}{n} \sum_{i=1}^n \frac{|x_{sim,i} - x_{obs,i}|}{x_{obs,i}}$$
 (22)

213 where $x_{sim,i}$ and $x_{obs,i}$ are the assimilated and observed model parameters for the i th month; \bar{x}_{sim}
214 and \bar{x}_{obs} are the mean of the assimilated and observed model parameters, respectively for the i th
215 month; n is the total number of data points.

216 3.2 Study area

217 3.2.1 Case 1: Wudinghe basin

218 The method is applied in the Wudinghe basin (**Fig. 1**) located in the southern fringe of Maowusu
219 Desert and the northern part of the Loess Plateau in China with a semiarid climate. It has a drainage
220 area of approximately 30,261 km² and a total length of 491 km and forms a part of the Yellow River
221 basin. The Wudinghe basin has an average slope of 0.2%, and its elevation ranges from 600 to 1800 m
222 above the sea level. The Baijiachuan gauge station, which is the most downstream station of the
223 Wudinghe basin, drains 98% of the total catchment area. The mean annual precipitation over the basin
224 is 401 mm, of which 72.5% occurs in the rainy season from June to September (**Fig. 2**). The mean
225 annual potential evapotranspiration is 1077 mm, and the mean annual runoff is about 39 mm with a
226 runoff coefficient of 0.1.

227



228 **3.2.2 Case 2: Tongtianhe basin**

229 The Tongtianhe basin (**Fig. 3**) is located in southwestern Qinghai Province in China with a continental
230 climate. It belongs to the source area of Yangtze River basin with a drainage area of about 140,000 km²
231 and a total main stream length of 1206 km. The elevation of the Tongtianhe basin approximately ranges
232 from 3500 to 6500 m above the sea level. Zhimenda is the basin outlet. The mean annual precipitation
233 over the basin is 440 mm, of which 76.9% occurs in the period from June to September (**Fig. 4**). The
234 mean annual potential evapotranspiration is 796 mm, and the mean annual runoff is about 99 mm with a
235 runoff coefficient of 0.23. The Tongtianhe basin is barely affected by human activities owing to the
236 limitation of the topographic condition and the water conservation measures conducted by the
237 government. It should be noted that the Tongtianhe basin is used for comparative study on model
238 parameter identification, where has no significant impacts from the climate change and human
239 activities.

240

241 **3.2.3 Data**

242 The data set including monthly precipitation, potential evapotranspiration and runoff in Wudinghe basin
243 (from 1956 to 2000) and Tongtianhe basin (from 1980 to 2013) are used in this study. The potential
244 evapotranspiration is estimated using the Penman-Monteith equation (Allen et al., 1998) based on the
245 meteorological data from the China Meteorological Data Sharing Service System (<http://cdc.nmic.cn>).



246 To reduce the impact of the model initial conditions, a 2-year data set, i.e., from 1956 to 1957 for
247 Wudinghe basin and from 1980 to 1981 for Tongtianhe basin, is reserved as the warm-up period. The
248 runoff estimations from the SCE-UA method (Duan et al., 1993) are compared with that of the EnKF.

249

250 **4 Results and discussion**

251 **4.1 Synthetic experiment**

252 To assess the performance of the EnKF, the assimilated results are examined for the four scenarios in
253 the synthetic experiment. The comparisons of the assimilated and true model parameters under
254 different scenarios are presented from **Fig. 5** to **Fig. 8**, and **Table 3** shows the evaluation statistics for
255 both the parameters and runoff assimilations. All these four figures show that the assimilated
256 parameters of C and SC have similar trends as the true ones. These figures demonstrate that the
257 SC assimilation performs better than the C assimilation. The runoff assimilation results (see **Table**
258 **3**, penultimate and last columns) show that the estimation of runoff using the EnKF perfectly matches
259 the observations with NSEs of 0.99 and VEs of approximately zero. It should be noted that there is a
260 time lag in assimilated C for the periodic case. In EnKF, the observation at the current time is used
261 to adjust the state variables and parameters, and the updates of parameters depend on the Kalman gain
262 for parameters.

263



264 The above results demonstrate that the EnKF is able to identify the temporal variation of the model
265 parameters by updating the state variable and parameters based on the runoff observations. The
266 estimated parameters for the cases of trend or abrupt change match the true values better than the case
267 with periodic variation.

268

269 4.2 Case studies

270 **Fig. 9** illustrates the double mass curve of monthly runoff and precipitation for Wudinghe and
271 Tongtianhe basins, respectively. The top panel shows the linear relationship between cumulative runoff
272 and precipitation before and after the turning point of January 1972 in the Wudinghe basin, which is
273 same as the result presented by Li et al. (2014). The results show two straight lines with different slopes
274 for the relationships between precipitation and runoff, indicating that changes occurred. While the
275 bottom panel demonstrates a single linear relationship fits all the data for the Tongtianhe basin,
276 suggesting a stable precipitation-runoff relationship during the 1982-2013 period.

277

278 The temporal variation of estimated SC and the associated 95% uncertainty interval are shown in **Fig.**
279 **10**. The top panel shows an apparent increasing trend with two stages in Wudinghe basin. The first stage
280 is from January 1958 to December 1971, when the water storage capacity has a significant increasing
281 trend with a slope of 0.059. The water storage capacity in the second stage, from January 1972 to



282 December 2000, has an obvious increasing trend with a slope of 0.022. The temporal variation of water
283 storage capacity is related to the change of catchment properties, such as the land use and land cover
284 change. Since the 1960s, the soil and water conservation measures, including tree and grass planting,
285 reservoir construction and land terracing, have been undertaken to cope with the soil erosion in
286 Wudinghe basin. During the 1970s, large-scale engineering measures were effectively implemented,
287 which improved the water holding capacity of the basin directly, and also provided a reasonable
288 physical explanation for the increasing trend and its degree of SC in the first stage. In the second stage,
289 the water storage capacity increases slower than the first stage since the engineering measures have
290 almost finished. Another important factor is the reduction of storage capacity for reservoirs caused by
291 sediment accumulation. In the 1980s, lots of measures were adopted for comprehensive management
292 within small catchments for further soil erosion control, which resulted in increasing grassland, forest
293 land and terracing land. These land use changes played a significant role in increasing water storage
294 capacity. On the other hand, the result of Tongtianhe basin shows that the estimated SC has no
295 pronounced trend since the R value has an insignificance level. Moreover, the range of variation in
296 estimated SC values is much smaller compared to those of the Wudinghe basin. The grey regions
297 represent the 95% uncertainty intervals obtained from the parameter ensemble. The results demonstrate
298 that the EnKF performs well for parameter estimation with narrow uncertainty bounds. **Fig. 11** shows
299 the temporal variation of estimated C values and the 95% uncertainty ranges for both Wudinghe basin



300 and Tongtianhe basin. The results demonstrate that the estimated C has a stable value, with slopes that
301 are almost zero for both the cases. The narrow uncertainty bounds indicate that the EnKF can provide
302 superior performance of parameter estimation.

303

304 **Fig. 12** illustrates the comparison of the observed and estimated runoff from the EnKF and SCE-UA for
305 both Wudinghe and Tongtianhe basins. The evaluation results are shown in **Table 4**. The NSEs from the
306 EnKF and SCE-UA in the Wudinghe basin are 0.93 and 0.16, and the VEs are 0.07 and 0, respectively.
307 While the corresponding index values from the EnKF and SCE-UA are 0.99 and 0.79, 0.04 and 0 in the
308 Tongtianhe basin. Therefore, the EnKF has superior performance compared to the SCE-UA for both
309 case studies. The results show that the data assimilation improves the runoff estimation.

310

311 In summary, these analyses show that the EnKF can identify the temporal variation of model parameters
312 well by updating both state variables and parameters based on the runoff observations. Moreover, the
313 trends of parameter SC can be explained by the change of catchment characteristics. On the contrary,
314 the estimated SC is approximately stable when the catchment is barely affected by human activities.
315 Consequently, the EnKF provides effective performance for time-variant parameter identification.

316

317 **5 Conclusions**



318 This study proposes an ensemble Kalman filter (EnKF) to identify the temporal variation of model
319 parameters in a monthly water balance. A synthetic experiment, which contains four scenarios of model
320 parameter variation, is designed to demonstrate the ability of the EnKF for identifying the temporal
321 variation of the model parameters using the runoff observations. The main conclusions are drawn as
322 follows.

323

324 Based on EnKF, the variation of model parameters can be effectively identified by assimilating runoff
325 observations. The EnKF can provide accurate results for parameter identification even though slight
326 time lags exist when parameters have periodic variations.

327

328 Then, the EnKF method is applied to the Wudinghe basin in China, aiming to detect the temporal
329 variability of model parameters and to provide an explanation for the parameter variation from the
330 perspective of catchment property change. Meanwhile, a comparative study is implemented to
331 investigate the variation of model parameters in Tongtianhe basin where human activities barely exist.
332 The parameter of water storage capacity (SC) for the monthly water balance model shows a significant
333 increasing trend for the period of 1958 to 2000 in the Wudinghe basin. The soil and water conservation
334 measures, including tree and grass planting, reservoir building and land terracing, have been
335 implemented during 1958 to 2000, resulting in the increase of the water holding capacity of the basin,



336 which explains the increasing trends of SC . Moreover, the magnitudes of the engineering measures in
337 different time periods play an important role in the degree of increasing trend for SC . In the Tongtianhe
338 basin, the parameter SC has no significant trend for the period of 1982 to 2013, which is consistent
339 with the relatively stationary catchment characteristics.

340

341 The method proposed in this paper provides an effective tool for the time-variant model parameters
342 identification. Future work will be focused on the influence of the correlations between/among model
343 parameters and performance comparison of multiple data assimilation methods.

344

345 **Acknowledgments**

346 This study was supported by the Excellent Young Scientist Foundation of NSFC (51422907). The
347 authors would like to thank the editor and the anonymous reviewers for their comments that helped
348 improve the quality of the paper.

349

350 **References**

- 351 Abaza, M., Anctil, F., Fortin, V., and Turcotte, R.: Sequential streamflow assimilation for short-term
352 hydrological ensemble forecasting, *J. Hydrol.*, 519, 2692-2706, doi:10.1016/j.jhydrol.2014.08.038,
353 2014.
- 354 Allen, R. G., Pereira, L. S., Raes, D., and Smith, M.: *Crop Evapotranspiration-Guidelines for*
355 *Computing Crop Water Requirements-FAO Irrigation and Drainage Paper 56*, Food and Agriculture
356 Organization of the United Nations, Rome, 1998.



- 357 Andréassian, V., Parent, E., and Michel, C.: A distribution-free test to detect gradual changes in
358 watershed behavior, *Water Resour. Res.*, 39, 1252, doi:10.1029/2003WR002081, 2003.
- 359 Brigode, P., Oudin, L., and Perrin, C.: Hydrological model parameter instability: A source of
360 additional uncertainty in estimating the hydrological impacts of climate change?, *J. Hydrol.*, 476,
361 410-425, doi:10.1016/j.jhydrol.2012.11.012, 2013.
- 362 Brown, A. E., Zhang, L., McMahon, T. A., Western, A. W., and Vertessy, R. A.: A review of paired
363 catchment studies for determining changes in water yield resulting from alterations in vegetation, *J.*
364 *Hydrol.*, 310, 28-61, doi:10.1016/j.jhydrol.2004.12.010, 2005.
- 365 DeChant, C. M. and Moradkhani, H.: Examining the effectiveness and robustness of sequential data
366 assimilation methods for quantification of uncertainty in hydrologic forecasting, *Water Resour. Res.*,
367 48, W04518, doi:10.1029/2011WR011011, 2012.
- 368 DeChant, C. M. and Moradkhani, H.: Toward a reliable prediction of seasonal forecast uncertainty:
369 Addressing model and initial condition uncertainty with ensemble data assimilation and sequential
370 Bayesian combination, *J. Hydrol.*, doi:10.1016/j.jhydrol.2014.05.045, 2014.
- 371 Delijani, E. B., Pishvaie, M. R., and Boozarjomehry, R. B.: Subsurface characterization with localized
372 ensemble Kalman filter employing adaptive thresholding, *Adv. Water Resour.*, 69, 181-196,
373 doi:10.1016/j.advwatres.2014.04.011, 2014.
- 374 Deng, C., Liu, P., Guo, S., Wang, H., and Wang, D.: Estimation of nonfluctuating reservoir inflow
375 from water level observations using methods based on flow continuity, *J. Hydrol.*,
376 doi:10.1016/j.jhydrol.2015.09.037, 2015.
- 377 Deng, C., Liu, P., Liu, Y., Wu, Z. H., and Wang, D.: Integrated hydrologic and reservoir routing model
378 for real-time water level forecasts, *J. Hydrol. Eng.*, 20(9), 05014032,
379 doi:10.1061/(ASCE)HE.1943-5584.0001138, 2015.
- 380 Duan, Q. Y., Gupta, V. K., and Sorooshian, S.: Shuffled complex evolution approach for effective and
381 efficient global minimization, *J. Optimiz. Theory App.*, 76, 501-521, doi:10.1007/bf00939380,
382 1993.
- 383 Guo, S., Chen, H., Zhang, H., Xiong, L., Liu, P., Pang, B., Wang, G., and Wang, Y.: A semi-distributed
384 monthly water balance model and its application in a climate change impact study in the middle and
385 lower Yellow River basin, *Water International*, 30, 250-260, doi:10.1080/02508060508691864,
386 2005.
- 387 Guo, S., Wang, J., Xiong, L., Ying, A., and Li, D.: A macro-scale and semi-distributed monthly water
388 balance model to predict climate change impacts in China, *J. Hydrol.*, 268, 1-15,
389 doi:10.1016/S0022-1694(02)00075-6, 2002.
- 390 Lü, H. S., Hou, T., Horton, R., Zhu, Y. H., Chen, X., Jia, Y. W., Wang, W., and Fu, X. L.: The
391 streamflow estimation using the Xinanjiang rainfall runoff model and dual state-parameter
392 estimation method, *J. Hydrol.*, 480, 102-114, doi:10.1016/j.jhydrol.2012.12.011, 2013.



- 393 Leisenring, M. and Moradkhani, H.: Analyzing the uncertainty of suspended sediment load prediction
394 using sequential data assimilation, *J. Hydrol.*, 468-469, 268-282, doi:10.1016/j.jhydrol.2012.08.049,
395 2012.
- 396 Li, S., Xiong, L., Dong, L., and Zhang, J.: Effects of the Three Gorges Reservoir on the hydrological
397 droughts at the downstream Yichang station during 2003–2011, *Hydrol. Processes* 27, 3981-3993,
398 doi:10.1002/hyp.9541, 2013.
- 399 Li, X.-N., Xie, P., Li, B.-B., and Zhang, B.: A probability calculation method for different grade
400 drought event under changing environment-Taking Wuding River basin as an example, *Shuili*
401 *Xuebao/Journal of Hydraulic Engineering*, 45, 585-594, doi:10.13243/j.cnki.slxb.2014.05.010,
402 2014.
- 403 Li, Z., Liu, P., Deng, C., Guo, S., He, P., and Wang, C.: Evaluation of the estimation of distribution
404 algorithm to calibrate a computationally intensive hydrologic model, *J. Hydrol. Eng.*,
405 doi:10.1061/(ASCE)HE.1943-5584.0001350, 2015.
- 406 Merz, R., Parajka, J., and Blöschl, G.: Time stability of catchment model parameters: Implications for
407 climate impact analyses, *Water Resour. Res.*, 47, W02531, doi:10.1029/2010WR009505, 2011.
- 408 Moradkhani, H., Sorooshian, S., Gupta, H. V., and Houser, P. R.: Dual state–parameter estimation of
409 hydrological models using ensemble Kalman filter, *Adv. Water Resour.*, 28, 135-147,
410 doi:10.1016/j.advwatres.2004.09.002, 2005.
- 411 Nash, J. E. and Sutcliffe, J. V.: River flow forecasting through conceptual models part I: A discussion
412 of principles, *J. Hydrol.*, 10, 282-290, doi:10.1016/0022-1694(70)90255-6, 1970.
- 413 Nie, S., Zhu, J., and Luo, Y.: Simultaneous estimation of land surface scheme states and parameters
414 using the ensemble Kalman filter: identical twin experiments, *Hydrol. Earth Syst. Sci.*, 15,
415 2437-2457, doi:10.5194/hess-15-2437-2011, 2011.
- 416 Paik, K., Kim, J. H., Kim, H. S., and Lee, D. R.: A conceptual rainfall-runoff model considering
417 seasonal variation, *Hydrol. Processes* 19, 3837-3850, doi:10.1002/hyp.5984, 2005.
- 418 Patil, S. D. and Stieglitz, M.: Comparing spatial and temporal transferability of hydrological model
419 parameters, *J. Hydrol.*, 525, 409-417, doi:10.1016/j.jhydrol.2015.04.003, 2015.
- 420 Samuel, J., Coulibaly, P., Dumedah, G., and Moradkhani, H.: Assessing model state and forecasts
421 variation in hydrologic data assimilation, *J. Hydrol.*, 513, 127-141,
422 doi:10.1016/j.jhydrol.2014.03.048, 2014.
- 423 Shi, Y., Davis, K. J., Zhang, F., Duffy, C. J., and Yu, X.: Parameter estimation of a physically based
424 land surface hydrologic model using the ensemble Kalman filter: A synthetic experiment, *Water*
425 *Resour. Res.*, 50, 706-724, doi:10.1002/2013WR014070, 2014.
- 426 Tamura, H., Bacopoulos, P., Wang, D., Hagen, S. C., and Kubatko, E. J.: State estimation of tidal
427 hydrodynamics using ensemble Kalman filter, *Adv. Water Resour.*, 63, 45-56,
428 doi:10.1016/j.advwatres.2013.11.002, 2014.



- 429 Vrugt, J. A., ter Braak, C. J. F., Diks, C. G. H., and Schoups, G.: Hydrologic data assimilation using
430 particle Markov chain Monte Carlo simulation: Theory, concepts and applications, *Adv. Water*
431 *Resour.*, 51, 457-478, doi:10.1016/j.advwatres.2012.04.002, 2013.
- 432 Wang, D., Chen, Y., and Cai, X.: State and parameter estimation of hydrologic models using the
433 constrained ensemble Kalman filter, *Water Resour. Res.*, 45, W11416, doi:10.1029/2008WR007401,
434 2009.
- 435 Westra, S., Thyer, M., Leonard, M., Kavetski, D., and Lambert, M.: A strategy for diagnosing and
436 interpreting hydrological model nonstationarity, *Water Resour. Res.*, 50, 5090-5113,
437 doi:10.1002/2013WR014719, 2014.
- 438 Xie, X. and Zhang, D.: Data assimilation for distributed hydrological catchment modeling via
439 ensemble Kalman filter, *Adv. Water Resour.*, 33, 678-690, doi:10.1016/j.advwatres.2010.03.012,
440 2010.
- 441 Xiong, L. and Guo, S.: Appraisal of Budyko formula in calculating long-term water balance in humid
442 watersheds of southern China, *Hydrol. Processes* 26, 1370-1378, doi:10.1002/hyp.8273, 2012.
- 443 Xiong, L. and Guo, S. L.: A two-parameter monthly water balance model and its application, *J.*
444 *Hydrol.*, 216, 111-123, doi:10.1016/S0022-1694(98)00297-2, 1999.
- 445 Xiong, L., Yu, K.-x., and Gottschalk, L.: Estimation of the distribution of annual runoff from climatic
446 variables using copulas, *Water Resour. Res.*, 50, 7134-7152, doi:10.1002/2013WR015159, 2014.
- 447 Xue, L. and Zhang, D.: A multimodel data assimilation framework via the ensemble Kalman filter,
448 *Water Resour. Res.*, 50, 4197-4219, doi:10.1002/2013WR014525, 2014.
- 449 Yan, H., DeChant, C. M., and Moradkhani, H.: Improving soil moisture profile prediction with the
450 particle filter-Markov chain Monte Carlo method, *IEEE Trans. Geosci. Remot. Sens.*, 53, 6134-6147,
451 doi:10.1109/tgrs.2015.2432067, 2015.
- 452 Ye, W., Bates, B. C., Viney, N. R., Sivapalan, M., and Jakeman, A. J.: Performance of conceptual
453 rainfall-runoff models in low-yielding ephemeral catchments, *Water Resour. Res.*, 33, 153-166,
454 doi:10.1029/96WR02840, 1997.
- 455 Zhang, D., Liu, X. M., Liu, C. M., and Bai, P.: Responses of runoff to climatic variation and human
456 activities in the Fenhe River, China, *Stoch. Environ. Res. Risk Assess.*, 27, 1293-1301,
457 doi:10.1007/s00477-012-0665-y, 2013.
- 458 Zhang, H., Huang, G. H., Wang, D., and Zhang, X.: Multi-period calibration of a semi-distributed
459 hydrological model based on hydroclimatic clustering, *Adv. Water Resour.*, 34, 1292-1303,
460 doi:10.1016/j.advwatres.2011.06.005, 2011.
- 461



462

463 Tables

464 **Table 1.** Description and prior ranges of the two parameters for the monthly water balance model.

| Parameters and state variable | | Description | Interval and unit |
|-------------------------------|------|----------------------------------|-------------------|
| Parameter | C | Evapotranspiration parameter | 0.2-2.0 (-) |
| | SC | Catchment water storage capacity | 100-2000 (mm) |
| State variable | S | Soil water content | mm |

465



466

467

Table 2. Scenarios of time-variant model parameters in the synthetic experiment.

| Scenario | Description |
|------------|---|
| Scenario 1 | C has a periodic variation, and SC has an increasing trend |
| Scenario 2 | C has a periodic variation, and SC has an abrupt change |
| Scenario 3 | C has a periodic variation with an increasing trend, and SC has an increasing trend |
| Scenario 4 | C has a periodic variation with an increasing trend, and SC has an abrupt change |

468



469

470

Table 3. Performance statistics for parameter and runoff estimations in the synthetic experiment.

| Scenario | Parameter | RMSE | R | MARE | NSE (Runoff) | VE (Runoff) |
|------------|-----------|--------|-------|------|-----------------|-------------|
| Scenario 1 | C | 0.15 | 0.554 | 0.21 | 0.99 | 0.0007 |
| | SC | 182.87 | 0.987 | 0.03 | | |
| Scenario 2 | C | 0.16 | 0.633 | 0.19 | 0.99 | 0.0001 |
| | SC | 156.19 | 0.957 | 0.04 | | |
| Scenario 3 | C | 0.12 | 0.636 | 0.12 | 0.99 | -0.0012 |
| | SC | 180.27 | 0.992 | 0.03 | | |
| Scenario 4 | C | 0.12 | 0.695 | 0.12 | 0.99 | -0.0009 |
| | SC | 156.42 | 0.969 | 0.03 | | |

471



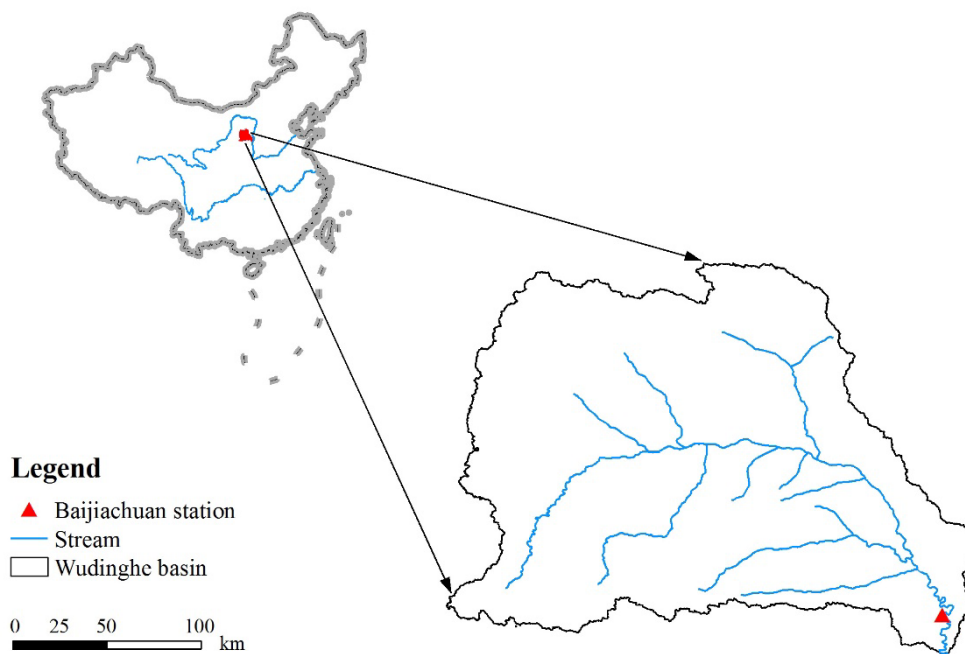
472

473 **Table 4.** Comparison of monthly runoff simulation performance between the optimization algorithm (SCE-UA) and
474 the data assimilation method (EnKF) in Wudinghe basin within the period 1958-2000 and Tongtianhe basin within
475 the period 1982-2013, respectively.

| Area | Method | NSE | VE |
|------------------|--------|------|------|
| Wudinghe basin | SCE-UA | 0.16 | 0 |
| | EnKF | 0.93 | 0.07 |
| Tongtianhe basin | SCE-UA | 0.79 | 0 |
| | EnKF | 0.99 | 0.04 |



476 **Figures**



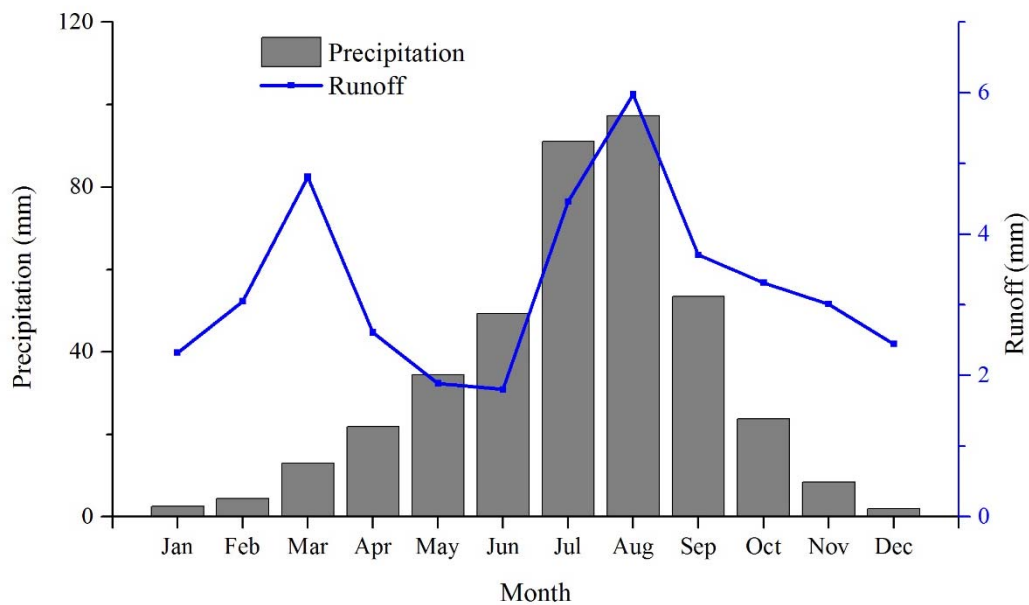
477

478

Figure. 1. Location of Wudinghe basin.



479



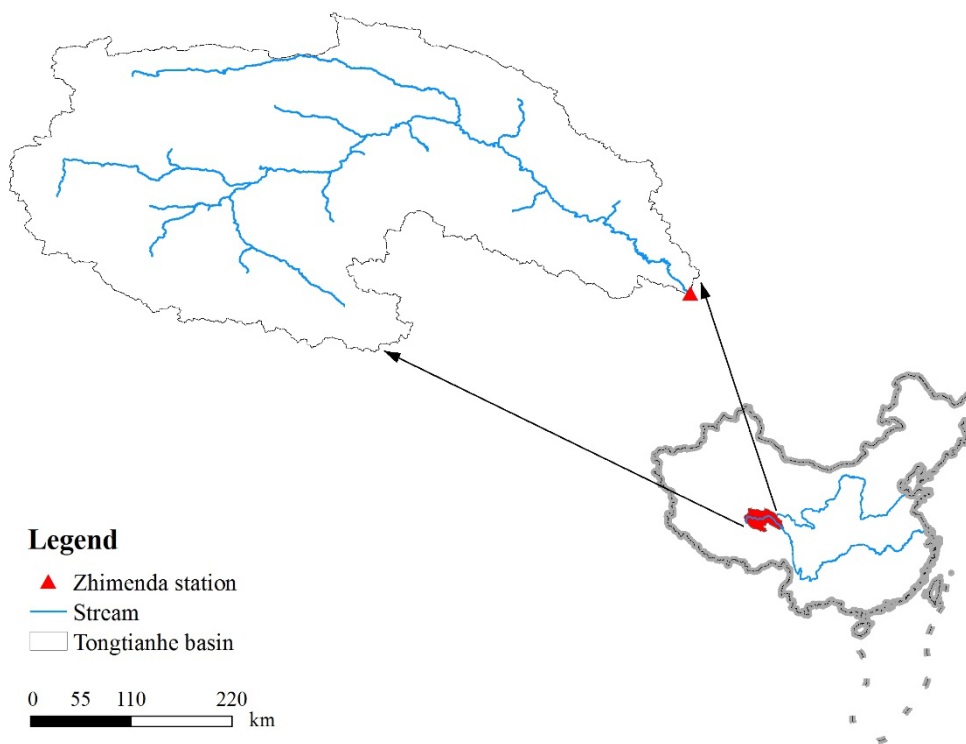
480

481

Figure 2. Mean monthly precipitation and runoff from 1956 to 2000 in Wudinghe basin.



482



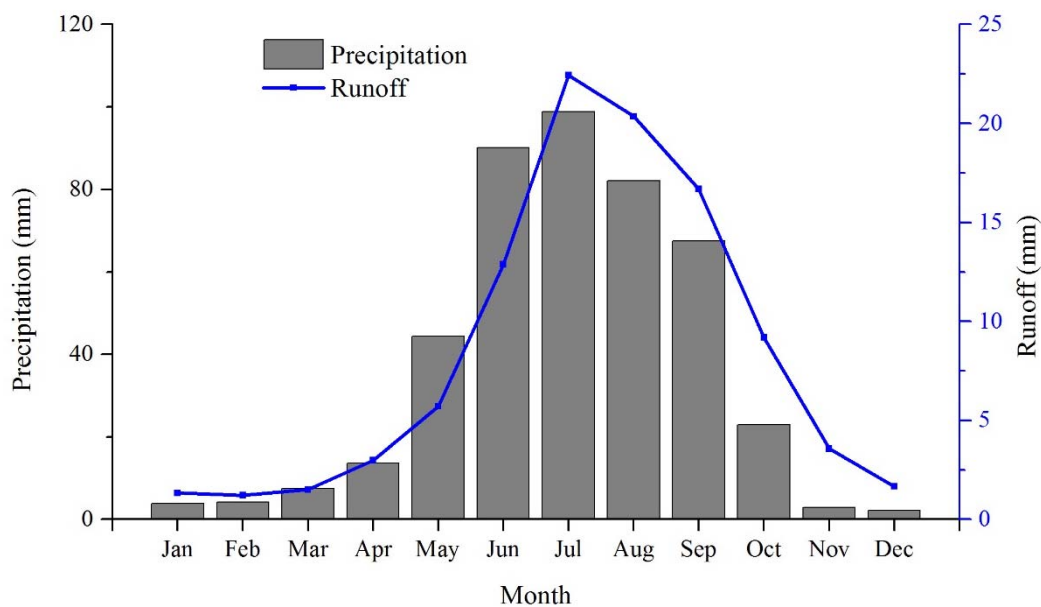
483

484

Figure. 3. Location of Tongtianhe basin.



485



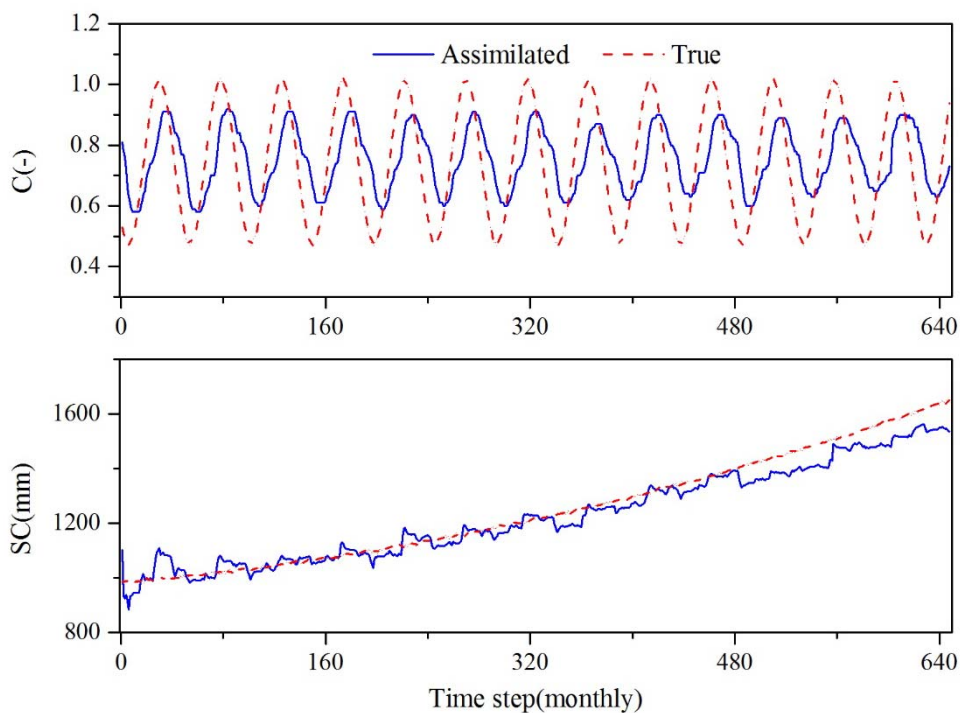
486

487

Figure 4. Mean monthly precipitation and runoff from 1980 to 2013 in Tongtianhe basin.



488



489

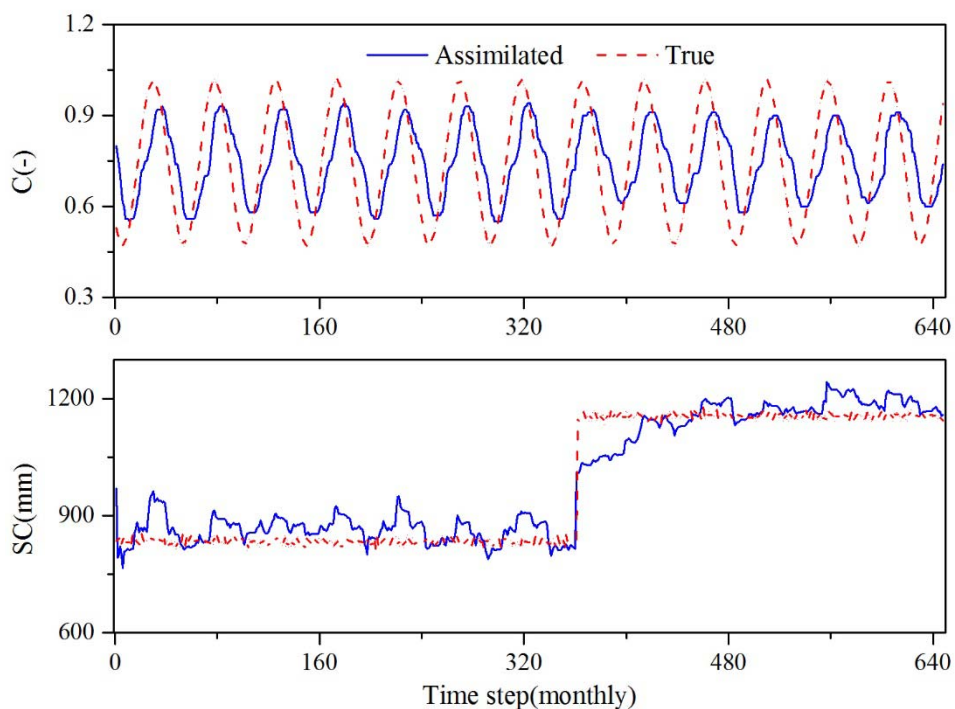
490

491

Figure 5. Model parameters (evapotranspiration parameter C , water storage capacity SC) of assimilated and true in the synthetic experiment, considering C and SC are periodicity and increasing trend, respectively.



492



493

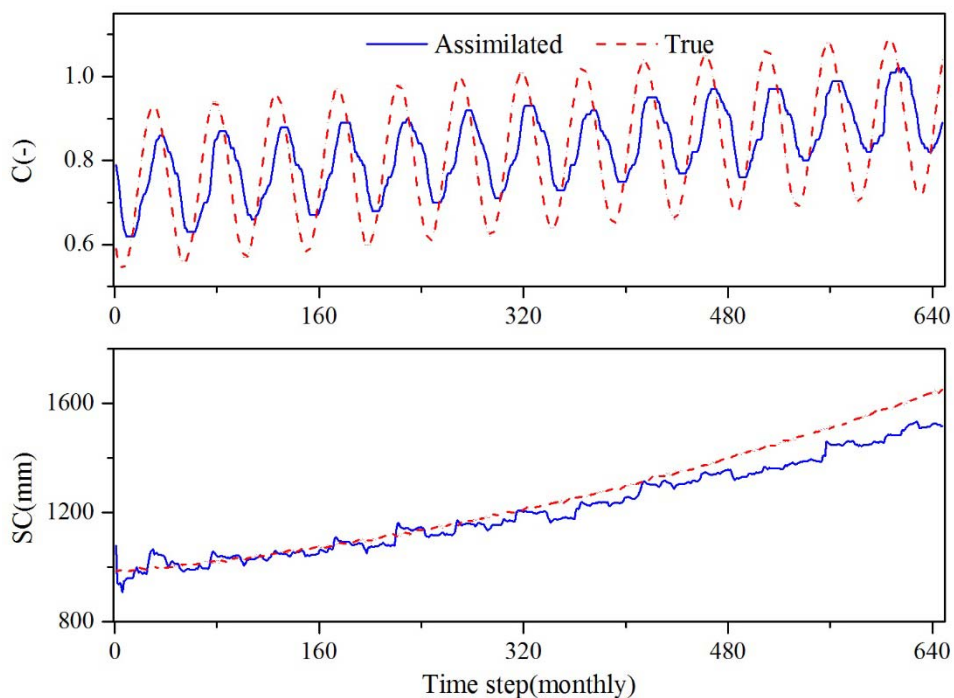
494

495

Figure 6. Model parameters (evapotranspiration parameter C , water storage capacity SC) of assimilated and true in the synthetic experiment, considering C and SC are periodicity and abrupt change, respectively.



496



497

498

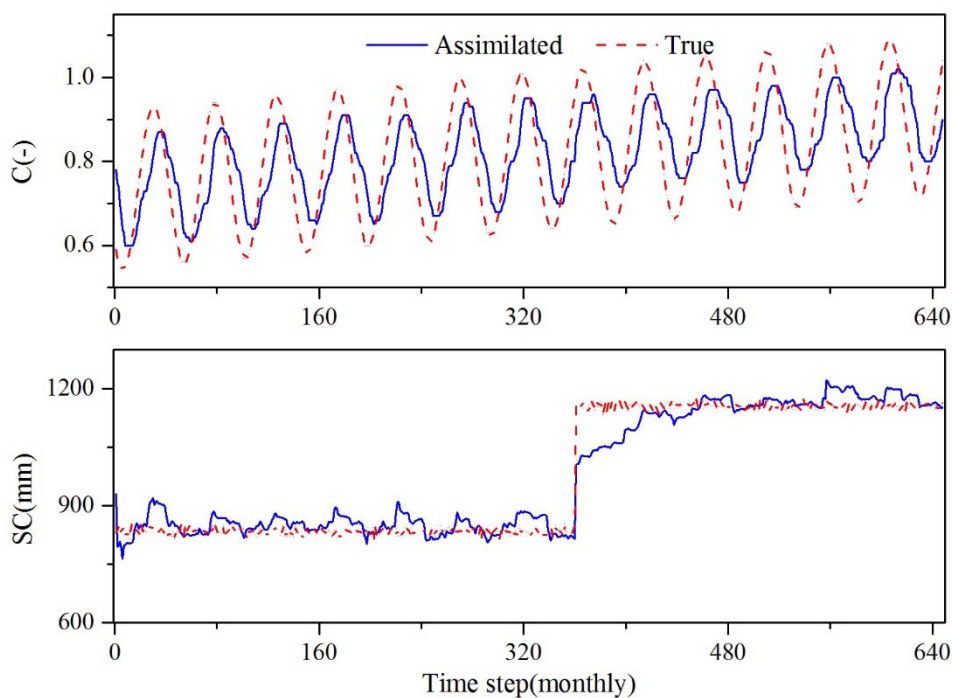
499

500

Figure. 7. Model parameters (evapotranspiration parameter C , water storage capacity SC) of assimilated and true in the synthetic experiment, considering C is periodicity with an increasing trend and SC is increasing trend, respectively.



501

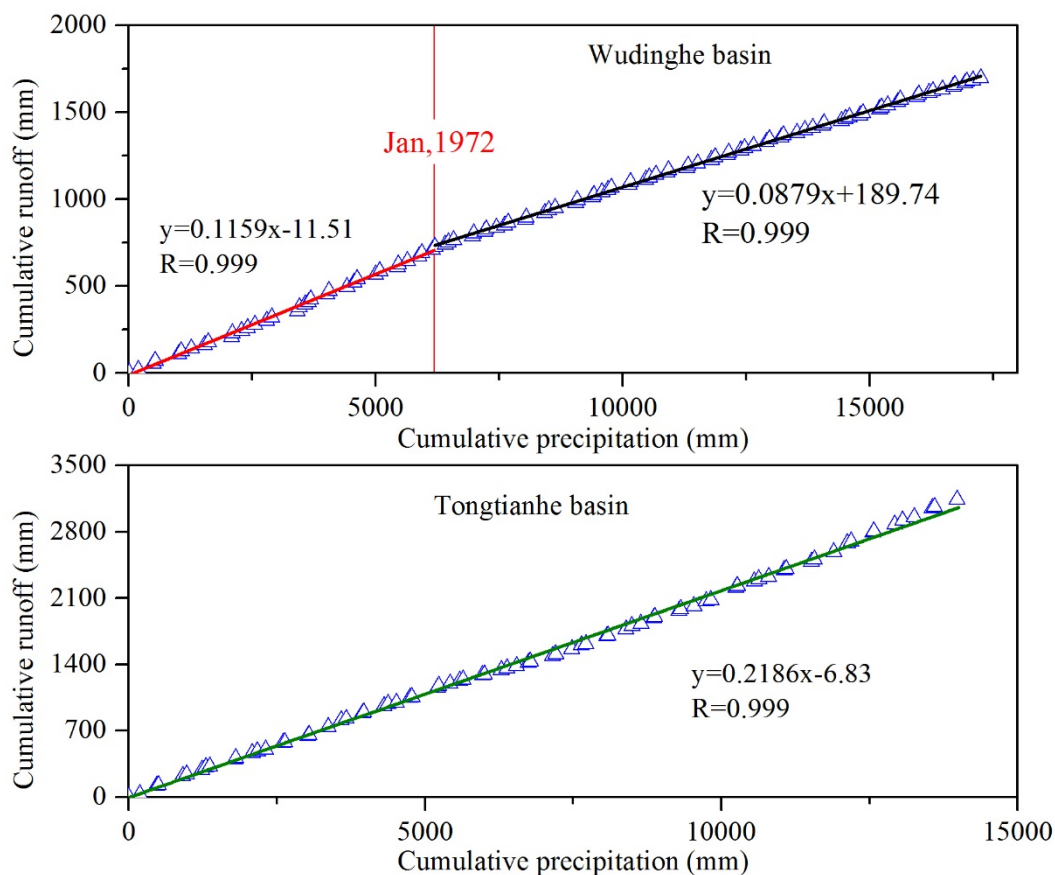


502

503 **Figure 8.** Model parameters (evapotranspiration parameter C , water storage capacity SC) of assimilated and true in
504 the synthetic experiment, considering C is periodicity with an increasing trend and SC is abrupt change, respectively.



505



506

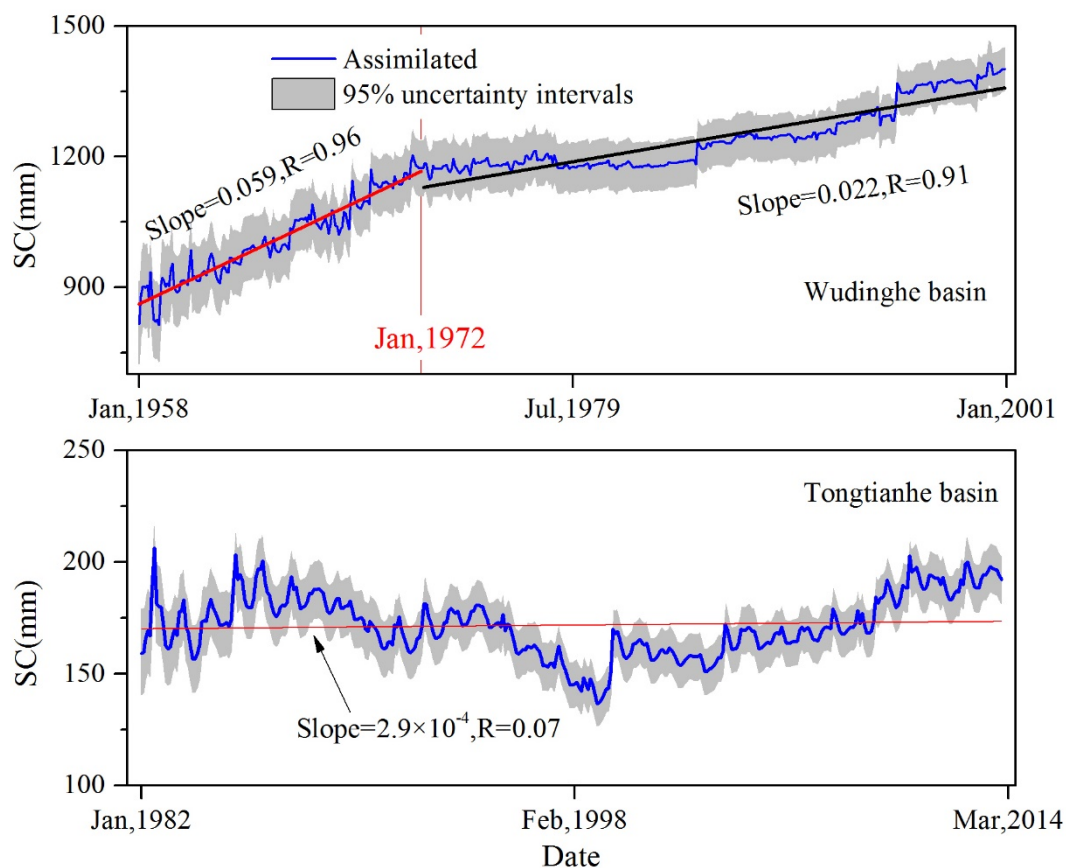
507

508

Figure. 9. Double mass curve of monthly runoff and precipitation for Wudinghe basin within the period 1958-2000 (top figure) and Tongtianhe basin within the period 1982-2013 (bottom), respectively.



509

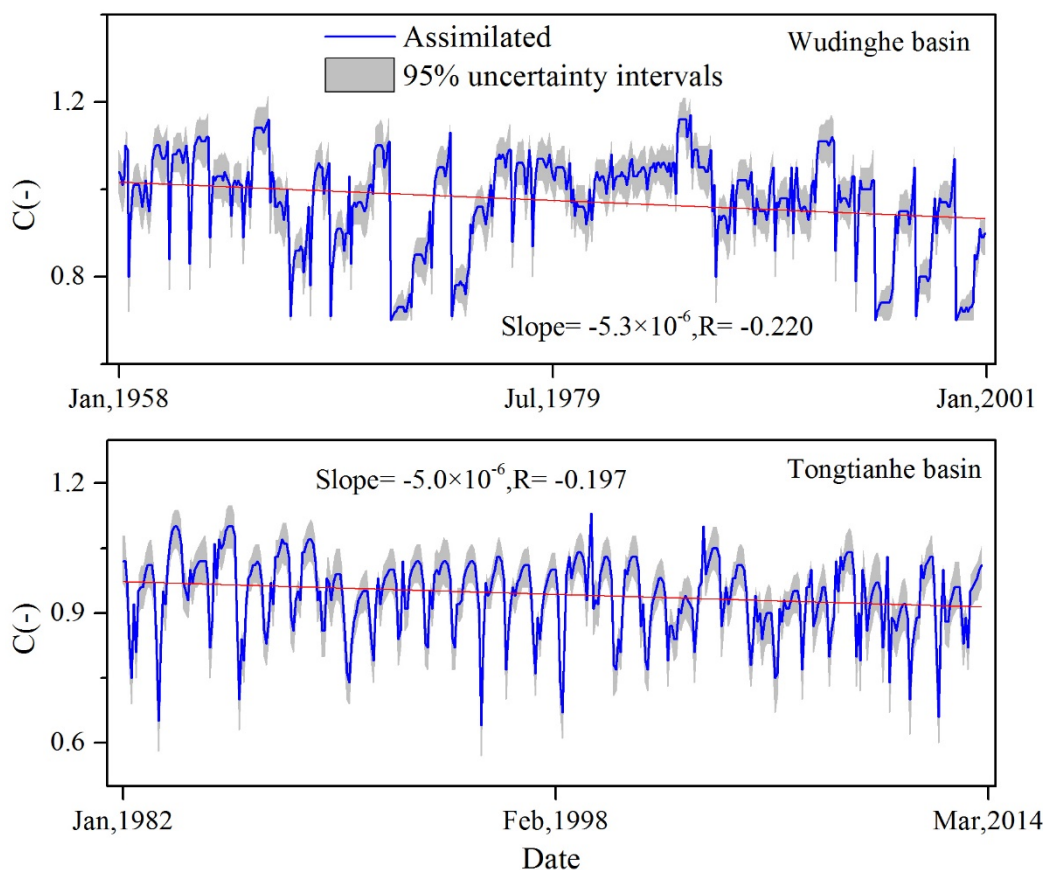


510

511 **Figure. 10.** Estimated parameter values of SC (water storage capacity) and associated 95% uncertainty intervals for
512 Wudinghe basin within the period 1958-2000 (top figure) and Tongtianhe basin within the period 1982-2013
513 (bottom).



514



515

516

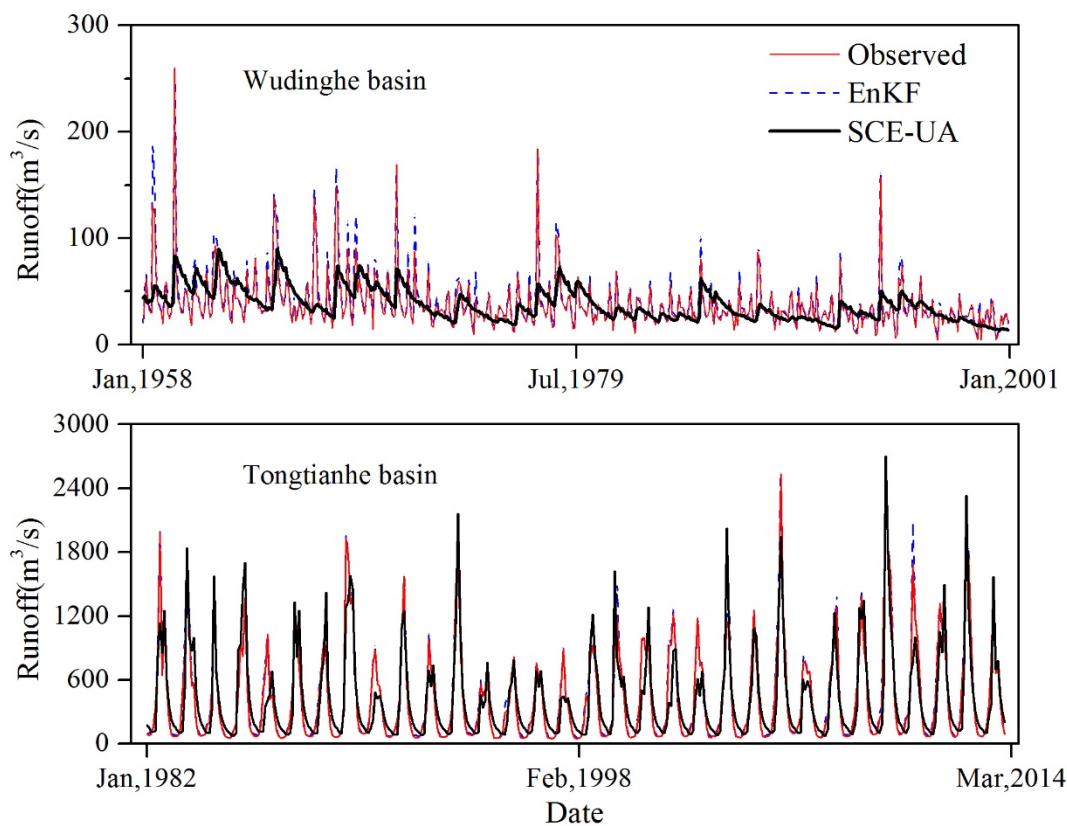
517

518

Figure. 11. Estimated parameter values of C (evapotranspiration parameter) and associated 95% uncertainty intervals for Wudinghe basin within the period 1958-2000 (top figure) and Tongtianhe basin within the period 1982-2013 (bottom).



519



520

521

522

Figure. 12. Comparison of observed runoff and runoff estimations from the EnKF and SCE-UA for Wudinghe basin within the period 1958-2000 (top figure) and Tongtianhe basin within the period 1982-2013 (bottom).